Thermal stability and magnetic properties of $MgFe_2O_4$@ZnO nanoparticles

Cite as: AIP Advances **7**, 056103 (2017); https://doi.org/10.1063/1.4975355
Submitted: 23 September 2016 . Accepted: 05 November 2016 . Published Online: 30 January 2017

S. Mallesh, D. Prabu, and V. Srinivas

Thermal stability and magnetic properties of $MgFe_2O_4$@ZnO nanoparticles

S. Mallesh,[1] D. Prabu,[2] and V. Srinivas[1]
[1]*Department of Physics, Indian Institute of Technology Madras, Chennai 600036, India*
[2]*Centre for Automotive Energy Materials, International Advanced Research Centre for Powder Metallurgy and New Materials, Chennai 600113, India*

(Presented 2 November 2016; received 23 September 2016; accepted 5 November 2016; published online 30 January 2017)

Magnesium ferrite, $MgFe_2O_4$, (MgFO) nanoparticles (NPs) have been synthesized through sol-gel process. Subsequently, as prepared particles were coated with Zinc-oxide (ZnO) layer(s) through ultrasonication process. Thermal stability, structure and magnetic properties of as-prepared (AP) and annealed samples in the temperature range of 350 °C-1200 °C have been investigated. Structural data suggests that AP MgFO NPs and samples annealed below 500 °C in air exhibit stable ferrite phase. However, α-Fe_2O_3 and a small fraction of MgO secondary phases appear along with ferrite phase on annealing in the temperatures range 500 °C- 1000 °C. This results in significant changes in magnetic moment for AP NPs 0.77 μ_B increases to 0.92 μ_B for 1200 °C air annealed sample. The magnetic properties decreased at intermediate temperatures due to the presence of secondary phases. On the other hand, pure ferrite phase could be stabilized with an optimum amount of ZnO coated MgFO NPs for samples annealed in the temperature range 500 °C-1000 °C with improvement in magnetic behavior compared to that of MgFO samples. [http://dx.doi.org/10.1063/1.4975355]

I. INTRODUCTION

Recently nanoparticles of $MgFe_2O_4$ (MgFO) spinel structures have been extensively investigated due to their low toxicity, good biocompatibility, magnetic behavior, low hysteresis loss and high density. These special features made them useful in wide range of potential applications, such as, sensors, catalysts, ferrofluids, and electromagnetic interference devices and in biological applications.[1–4] The MgFO belongs to the cubic inverse spinel (AB_2O_4) structure with Fd-3m space group, where A, B are the tetrahedral and octahedral sites of cations respectively. The general distribution of cations can be expressed as $(Mg^{2+}{}_{1-\delta}Fe^{3+}{}_{\delta})_{tet}[Mg^{3+}{}_{\delta}Fe^{3+}{}_{2-\delta}]_{oct}$, where δ is an inversion parameter, which varies from 0 (normal spinel) to 1(inverse spinel). In general, for bulk Mg-ferrite δ is observed to be 0.9 and it varies significantly for NPs.[5] In Mg-ferrite magnetization arises from the antiparallel alignment of Fe^{3+} at tetrahedral and octahedral sites respectively. Therefore the magnetic properties depend on distribution of cations, which intern depends on the method of synthesis and processing conditions.[1,5,6] Several groups have investigated the physical and chemical properties of MgFO NPs synthesized by different methods, such as, mechano-chemical rout[1] high energy ball milling,[5] co-precipitation method,[7] micro emulsion,[8] and sol-gel process[9] and subjected to heat treatment in order to study the structure and magnetic properties. Recent observations suggest that the nano MgFO, when annealed in the temperature range of 500 °C- 1000 °C the ferrite phase is unstable and degrades into secondary phases, such as, MgO, Fe_2O_3 along with the ferrite phase, which causes deterioration of magnetic properties of MgFO.[1,9,10] Similar behavior was also observed in MnZn ferrite nanoparticles when annealed in the temperatures 600 °C- 1000 °C exhibit secondary phases like Fe_2O_3, Mn_2O_3 etc.[11] However, stabilization of ferrite phase at lower annealing temperatures is important to retain the low dimensional character of the material. Ichiyanag et al., have observed amorphous phase in silica coated MgFO when annealing below 800 °C.[12] Thermal stability, structure

and magnetic properties of ZnO coated and uncoated MnZn ferrite NPs have been investigated earlier.[13,14] From these studies it was suggested that the ZnO coating can protect the ferrite phase form oxidation. The ZnO is a wide band-gap II–IV semiconductor, which is chemically thermally stable, useful to reduce the agglomeration and prevent oxidation of ferrite particles. The ZnO with ferrite NPs can improve their optical properties and make them suitable for magneto-optic, spintronic devices as well as biomedical applications.[15] The $MgFe_2O_4$–ZnO composites were investigated for magnetic and photo-catalytic performance.[16] The photo-catalytic performance was enhanced in $MgFe_2O_4$–ZnO heterojunctions.[17] In this work the effect of ZnO coating layer on MgFO NPs has been investigated to see (i) whether the fraction of impurity phases can be reduced on low temperature annealing? (ii) is ZnO layer stable on low temperature annealing? (iii) how are the magnetic and structural properties modified?

II. EXPERIMENTAL DETAILS

The MgFO nanoparticles were synthesized via sol-gel method as reported in the earlier work.[13] Subsequently required amount of Zinc acetate, $Zn(CH_3COO)_2.2H_2O$, is dissolved in millipore distilled water and MgFO NPs were dispersed in this solution. The pH maintained at 8.0 by drop wise addition of NaOH solution. Subsequently, the solution was ultrasonicated for one hour to overcome the agglomerations and to encapsulate ZnO on the surface of the particles. The precipitate was washed several times with de-ionized water and dried at 70 °C. All the as-prepared powder samples were annealed at 350 °C-1200 °C in air to evaluate the thermal stability and magnetic properties. The structure and thermal stability was investigated using X-ray diffraction (XRD) data, which was collected at room temperature (RT) in the angular range of 20-80° with 0.016 step by using CuKα (λ=1.54059Å) radiation in a PANalytical (X'pert PRO). The structure and crystallographic phases of samples were analyzed by Rietveld refinement using GSAS software. Raman spectra (Jobin-Yvon LabRAM HR800UV spectrometer with 633 nm emission line of an He-Ne laser) was collected at RT. The magnetic measurements were carried out by using a Microsense EV9 vibrating sample magnetometer (VSM) at RT.

III. RESULTS AND DISCUSSIONS

Fig. 1 (a) shows Rietveld refinement of XRD patterns of AP and annealed MgFO powders. The structural parameters obtained from the XRD data are summarized in Table I As prepared NPs exhibit single phase spinel structure and ferrite phase is observed to be stable when annealed at 350 °C. However, evolution of α-Fe_2O_3 and small fraction of MgO secondary phases were observed along with ferrite phase when the samples were annealed in the temperature range of 500 °C -1000 °C. The weight fraction of secondary phases is maximum for the sample annealed at 600 °C, interestingly enough when samples are annealed at temperature greater than 600 °C the weight fraction of secondary phases decreased. Further it is also observed that the impurity phases appear to dissolve above 1000 °C and a pure stable ferrite phase reappears on annealing at 1100-1200 °C in air for 12h.

$$MgFe_2O_4 + 1/2[O_2] \underset{1100-1200\,^\circ C}{\overset{500-1000\,^\circ C}{\rightleftharpoons}} Fe_2O_3 + MgO. \quad (1)$$

This indicates that at elevated temperatures secondary phases react together to form ferrite phase like as in solid state reaction. The AP NPs exhibit broad XRD peaks and which become sharper with annealing temperature indicating a significant increase in crystallite size at elevated temperatures. The crystallite size is estimated from XRD peak broadening employing Scherrer formula. The average crystallite size observed to be 12 nm for AP NPs is essentially constant up to 700 °C. Above this temperature crystallite size increases with annealing temperature and approaches bulk value for sample annealed at 1200 °C. The lattice parameter 8.3830(3) Å for AP NPs essentially increases to 8.3965(2) for 800 °C annealed sample and then decreases to 8.3867(4) Å for 1200 °C annealed samples (Table I). Significant changes were observed in crystallite size and lattice parameters with annealing temperatures. The observed results are in agreement with earlier reports.[9] However

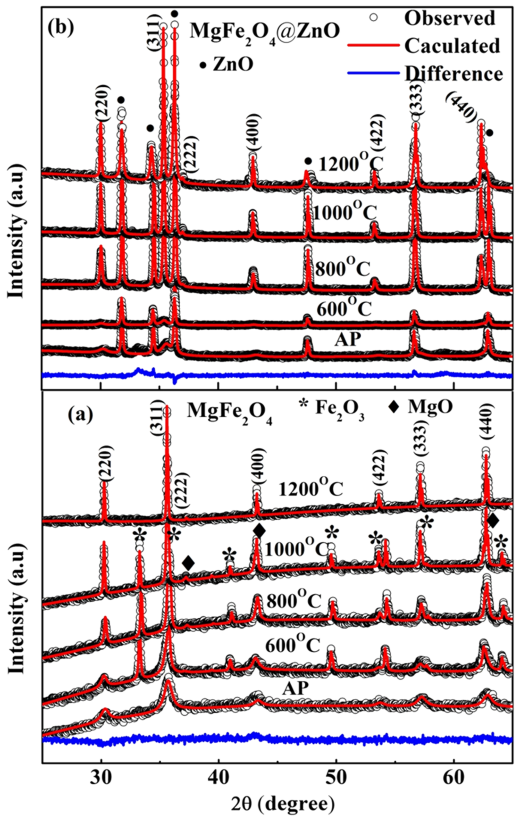

FIG. 1. Rietveld refinement of XRD patterns of (a) MgFO, (b) MgFO@ZnO (x=0.6) AP and air annealed samples respectively.

TABLE I. The structural parameters obtained from Rietveld refinement for MgFO as-prepared and air annealed samples respectively. T_a and t represent annealing temperature and crystallite size respectively.

Samples		Lattice constants				wt (%)			
		Spinel	α- Fe_2O_3		MgO				
T_a	T (nm)	a (Å)	a=b (Å)	c (Å)	a (Å)	Spinel	α-Fe_2O_3	MgO	χ^2
As-prepared	11	8.3830(8)	-	-	-	100	-	-	1.08
500°C	13	8.3848(7)	5.0389(8)	13.775(4)	-	85.7(8)	14.2(6)	-	1.02
600°C	15	8.3898(8)	5.0374(4)	13.757(2)	4.2092(8)	49.2(6)	35.8(4)	14.9(5)	1.08
700°C	16	8.3950(3)	5.0390(3)	13.767(2)	4.2127(7)	50.2(5)	33.4(6)	16.3(4)	1.42
800°C	43	8.3965(2)	5.0405(2)	13.760(8)	4.2093(3)	51.3(7)	30.7(5)	18.3(3)	1.06
900°C	65	8.3899(3)	5.0376(2)	13.756(6)	4.2098(3)	54.4(5)	29.3(7)	16.2(5)	1.12
1000°C	113	8.3866(2)	5.0374(2)	13.750(4)	4.2081(3)	62.4(4)	19.6(8)	17.6(2)	1.37
1200°C	Bulk	8.3867(4)	-	-	-	100	-	-	1.25

stabilization of ferrite phase is essential at intermediate temperatures to retain the nanophase characteristics. Therefore to stabilize the ferrite phase at intermediate temperatures, we have coated ZnO on MgFO NPs with $(MgFe_2O_4)_{1-x}/(ZnO)_x$ (x=0, 0.3, 0.5 & 0.6) compositions. As the thickness of ZnO layer increases on the surface of MgFO NPs, the fraction of secondary phases decreases when samples are annealed at 600 °C in air. It is observed that the ferrite phase stabilized for x=0.6 concentration. Further annealing at temperatures 800-1200 °C x=0.3 and 0.5 concentrations exhibit pure ferrite phase. Fig. 1(b) shows Reitveld refinement of XRD patterns of AP and air annealed MgFO@ZnO samples for x=0.6. The AP NPs exhibit ferrite and ZnO composite phase with no impurity phases

TABLE II. The structural parameters obtained from Rietveld refinement for MgFO@ZnO (x=0.6) as-prepared and air annealed samples respectively.

Samples		Lattice constants			wt (%)		
		Spinel	ZnO				
T_a	T (nm)	a (Å)	a=b (Å)	c (Å)	Spinel	ZnO	χ^2
As-prepared	10	8.3823(7)	3.2494(1)	5.2019(2)	62.1(6)	37.9(4)	1.73
600°C	15	8.4097(8)	3.2486(8)	5.2036(4)	66.4(8)	33.2(5)	1.77
800°C	57	8.4118(4)	3.2523(7)	5.2052(7)	73.1(7)	26.9(8)	1.95
1000°C	114	8.4130(2)	3.2539(3)	5.2013(6)	75.4(4)	24.6(6)	2.05
1200°C	bulk	8.4142(4)	3.2542(4)	5.2028(5)	77.2(2)	22.8(4)	1.51

for all annealing temperatures (600 °C -1200 °C). The results obtained from structural analysis are shown in Table II. The fraction of ferrite phase increased by decreasing ZnO phase with annealing temperature which clearly indicates that during the annealing the interfacial (MgFO@ZnO) reaction takes place, This probably leads to formation of MgZn ferrite phase at the interface. The crystallite size and lattice parameter increases with increasing of annealing temperature. The distribution of cations varies with annealing temperature which intern affects the lattice parameter. The cationic radius of Zn^{2+} (0.82Å) is greater than the Mg^{2+} (0.78 Å) and hence it is possible that the lattice parameter increases as the Zn is placed into Mg sites. The Rietveld refinement of XRD data confirms the ferrite phase belongs to the cubic spinel structure with Fd-3m space group (JCPDS file No. 88-1943). The α-Fe_2O_3, MgO phases have rhombohedral crystal structure with R-3c space group (JCPDS file No. 33-0664) and cubic crystal structure with Fm-3m space group (JCPDS file

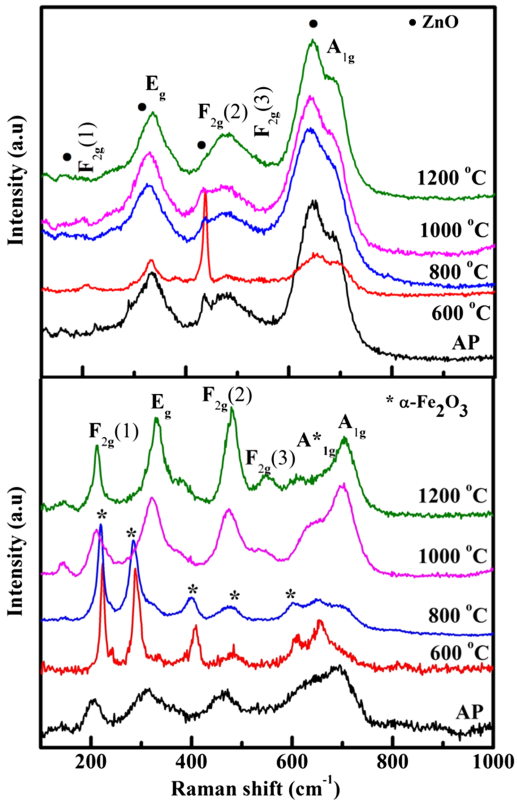

FIG. 2. Raman spectra of (a) MgFO, (b) MgFO@ZnO (x=0.6) AP and air annealed samples respectively.

No. 87-0653) respectivily. The ZnO phase is hexagonal crystal structure with P63mc space group (JCPDS file No. 36-1451).

In order to study the vibrational properties of the pure and secondary phases of samples Raman spectra is recorded at room temperature in the frequency range from 100-1000 cm^{-1}. Fig. 2(a) shows the Raman spectra of AP NPs and air annealed MgFO samples respectively. The AP NPs and 1200 °C in air annealed samples exhibit pure ferrite Raman active modes. The ferrite modes of AP NPs are weak compared to that of 1200 °C annealed samples, which could be due to strain and disorder on surface of the NPs. The ferrite modes observed A_{1g} (691- 705 cm^{-1}) $3F_{2g}$ (531-548, 467-482, 207 -212 cm^{-1}) and E_g (312-330 cm^{-1}) respectively. The ferrite modes were shifted to higher frequencies with annealing temperature. The Fe_2O_3 modes were detected in air annealed (500-1000 °C) samples. The corresponding Fe_2O_3 modes A_{1g}, $E_g(2)$ and $E_g(4)$ detected in Raman spectra are 218-226 cm^{-1}, 280-288 cm^{-1} and 398-408 cm^{-1} respectively. The Fe_2O_3 modes were shifted to lower frequencies with annealing temperature. The observations on XRD and Raman spectra suggest that some amount of MgO impurity phase may be present in samples but the dominant impurity phase is Fe_2O_3. It is further confirmed from Raman spectra that mainly Fe_2O_3 evolves from Mg ferrite at intermediate temperatures (500-1000°C). Fig. 2(b) shows the Raman spectra of AP NPs and annealed MgFO@ZnO samples respectively. The Raman spectra of MgFO@ZnO samples exhibit pure ferrite modes along with ZnO modes. The ferrite modes observed A_{1g} (680- 690cm^{-1}) $3F_{2g}$ (520-537, 472-480, 190 -200 cm^{-1}) and E_g (330-335 cm^{-1}) respectively. The modes were corresponding ZnO are $2E_1$(low), E_2(low), E_2(high), A1(high) detected in Raman spectra are 159-160 cm^{-1}, 290-310 cm^{-1} and 430 -437 cm^{-1}, 640-650 cm^{-1} respectively.[18] The XRD and Raman studies indicate that ZnO shell protects ferrite phase from oxidation during annealing at intermediate temperatures.

Magnetization (M) measured as function of magnetic field (H) at room temperature is shown in fig. 3 for AP and air annealed MgFO, MgFO@ZnO samples respectively. The AP MgFO samples show lower saturation magnetization (M_s) ~21 emu/g, in spinal ferrite phase. Further they exhibit saturation at higher magnetic field values compared to that of sample annealed at 1200 °C. This difference can be attributed to the presence of strain and disorder in NPs. The samples annealed at higher temperatures exhibit magnetic behavior which corroborates well with the XRD shown in fig. 1. The 600 °C air annealed samples exhibits weak magnetic moment (~11 emu/g) due to the presence

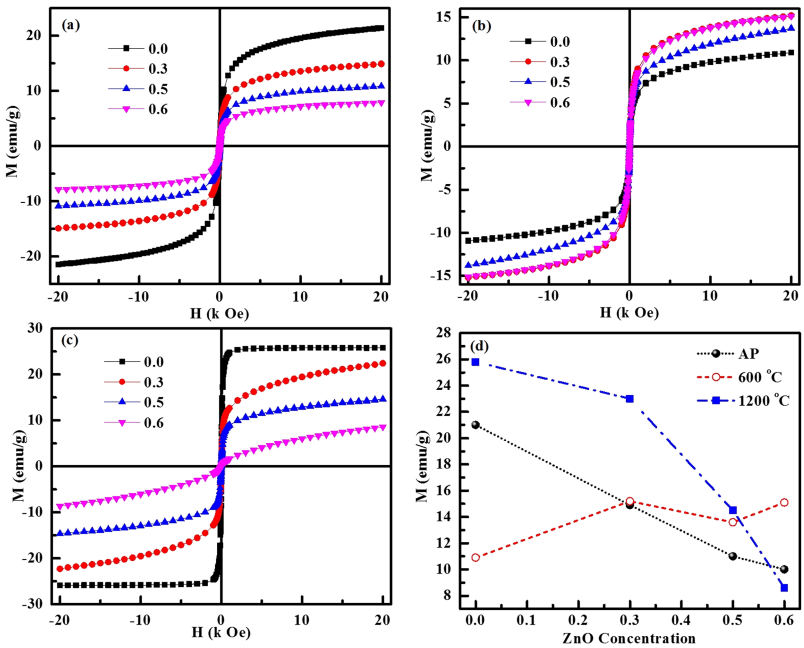

FIG. 3. M-H curves of MgFO and ZnO coated MgFO (a) AP, (b) 600 °C, (c) 1200 °C air annealed samples respectively. (d) Magnetization as function of ZnO concentration.

of impurity phases (α-Fe_2O_3 and MgO). On increasing the annealing temperature from 600 °C to 1200 °C, magnetization increases systematically and reaches a value of 25.8 emu/g. This is due to the increases of spinel phase at the expense of impurity phases. These observations corroborate well with structural data and suggest that the annealing temperature plays a crucial role in controlling the impurity phases. On the other hand magnetization of AP MgFO@ZnO samples decreases with ZnO concentration. The M increases to 14-16 emu/g for sample annealed at 600 °C. This increase in magnetization is due stable ferrite phase in the presence of ZnO layer. Further magnetization rapidly decrease (26-9 emu/g) for samples annealed at 1200 °C. Even though the ferrite phase is stable at all annealing temperature, but magnetization values are lower compared to that of MgFO samples, which might be due the presence of nonmagnetic ZnO in ferrite phase. The non-saturation of magnetization at higher applied fields could be due to the formation of MgZn ferrite phase at the interface of MgFO@ZnO. The bulk Zn-ferrite is paramagnetic at room temperature with antiferromagnetically ordered below 10K.[19] The magnetizations data corroborate well with structural data suggest that the interfacial (MgFO@ZnO) reaction plays a crucial role on magnetic behavior of the samples.

The net magnetic moment in Mg-ferrite is from the antiparallel alignment of Fe^{3+} ions at A and B sublattices respectively. It has been observed from the experiments that the saturation magnetic moment (M_B) at B site is greater than that of A site magnetic moment (M_A). Therefore the resultant saturation magnetization can be written as

$$M_s = |M_B - M_A| . \tag{2}$$

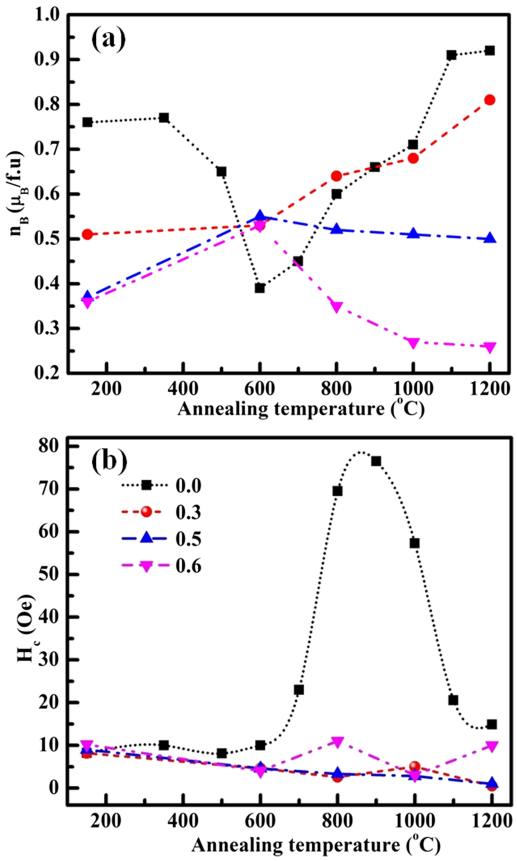

FIG. 4. Comparison of (a) Magnetic moment n_B per formula unit and (b) Coercivity as a function of annealing temperature for MgFO, ZnO coated MgFO samples respectively.

The magnetic moment per formula unit can be calculated by the following equation

$$n_B = \frac{Mol.wt \times M_s}{5585}. \quad (3)$$

Where n_B is the magnetic moment (Bohr magnetons) and M_s is the saturation magnetization calculated per gram at 300K. Fig. 4(a) shows the magnetic moment per formula unit as a function of annealing temperature for MgFO, MgFO@ZnO samples respectively. For MgFO the calculated n_B for *AP* nanoparticles is 0.77μ_B decreases initially to 0.39 μ_B for 600 °C air annealed sample due to the presence of secondary phases. Further magnetic moment increases with the increase in annealing temperature and it reaches to 0.92 μ_B for 1200 °C air annealed sample. On the other hand n_B is 0.53μ_B for 600 °C annealed MgFO@ZnO (x=0.3) sample increases to 0.81μ_B for 1200 °C air annealed sample. Similarly n_B is 0.53μ_B for 600 °C annealed MgFO@ZnO (x=0.6) sample but decreases to 0.26 μ_B for 1200 °C air annealed sample. The lower magnetic moment for MgFO@ZnO sample compared to MgFO samples is due to the presence of nonmagnetic ZnO. The maximum coercivity (H_c) 76.5 Oe is observed for MgFO sample annealed at 900 °C, which is due to the evolution of secondary phase (α-Fe_2O_3). The H_c decreases above and below 900 °C as shown in Fig. 4(b). The H_c (<10 Oe) significantly decreased in MgFO@ZnO samples compared to that of MgFO samples. These magnetic measurements corroborate well with the structural data. Therefore, from present study we suggest an optimum ZnO (x=0.3) coating on MgFO enables us to contain the α-Fe_2O_3 phase with reasonable magnetic moment.

IV. CONCLUSIONS

The XRD patterns of as prepared and annealed nanoparticles of $MgFe_2O_4$ samples shows pure spinel phase. But annealing at intermediate temperature (500 °C- 1000 °C) results in evolution of α-Fe_2O_3, MgO secondary phases along with ferrite phase. This results in deterioration magnetic properties. On the other hand pure ferrite phase is stabilized in ZnO coated on MgFO NPs at all annealing temperature (600 °C-1200 °C). It has been shown that the annealing temperature plays an important role on evolution of impurity phases (α-Fe_2O_3, MgO). Further it is also demonstrated that impurity phase can be contained by encapsulation of optimum ZnO layers. The structure and magnetization studies indicate that there is an interfacial (MgFO@ZnO) reaction during annealing, which probably leads to the formation of MgZn ferrite phase in the interface region.

[1] B. Antic, N. Jovic, M. B. Pavlovic, A. Kremenovic, D. Manojlovic, M. V. Vasic, and A. S. Nikolic, J. Appl Phys. **107**, 043525 (2010).
[2] M. Shahid, L. Jingling, Z. ali, I. Shakir, M. F. Warsi, R. Parveen, and M. Nadeem, Mater. Chem. Phys. **139**, 566 (2013).
[3] G. Yang, X. Li, Z. Zhao, and W. Wang, Acta. Pharmacol. Sin. **30**, 1688 (2009).
[4] V. M. Khot, A. B. Salunkhe, N. D. Thorat, R. S. Ningthoujam, and S. H. Pawar, Dalton Trans. **42**, 1249 (2013).
[5] V. Sepelak, A. Feldhoff, P. Heitjans, F. Krumeich, D. Menzel, F. J. Litterst, I. Bergmann, and K. D. Becker, Chem. Mater. **18**, 3057 (2006).
[6] A. A. Thant, S. Srimala, P. Kaung, M. Itoh, O. Radzali, and M. N. Ahmad Fauzi, J. Aust. Ceram. Soc. **46**, 11 (2010).
[7] L. Zhang, X. Zhou, X. Guo, X. Song, and X. Liu, J. Mol. Catal. A. Chem. **335**, 31 (2011).
[8] P. Holec, J. Plocek, D. Niznansky, and J. P. Vejpravova, J. Sol-gel Sci Technol. **51**, 301 (2009).
[9] A. C. Druc, A. M. Dumitrescu, A. I. Borhan, V. Nica, A. R. Iordan, and M. N. Palamaru, Cent. Eur. J. Chem. **11**, 1330 (2013).
[10] T. P. Sumangala, C. Mahender, B. N. Sahu, N. Venkataramani, and S. Prasad, Physica B. **448**, 312 (2014).
[11] A. Angermann, J. Topfer, K. L. da Silva, and K. D. Becker, J. Alloys Compd. **508**, 433 (2010).
[12] Y. Ichiyanagi, M. Kubota, S. Moritake, Y. Kanazawa, T. Yamada, and T. Uehashi, J. Magn. Magn. Mater. **310**, 2378 (2007).
[13] S. Mallesh, S. Kavita, R. Gopalan, and V. Srinivas, IEEE Trans. Magn. **50**, 2008204 (2014).
[14] S. Mallesh, A. Sunny, M. Vasundhara, and V. Srinivas, J. Magn. Magn. Mater. **418**, 112 (2016).
[15] S. Wang, X. Gao, J. Yang, Z. Zhu, H. Zhang, and Y. Wang, RSC Adv. **4**, 57967 (2014).
[16] G. Nabiyouni, D. Ghanbari, J. Ghasemi, and A. Yousofnejad, J. Nano. Struct. **5**, 289 (2015).
[17] N. R. Su, L. Pin, M. Li, X. Zhang, M. Li, and J. Niu, Mater. Lett. **122**, 201 (2014).
[18] K. Mahamood, S. B. Park, and H. J. Sung, J. Mater. Chem. C. **1**, 3138 (2013).
[19] J. M. Hastings and L. M. Corliss, Phys. Rev. **102**, 1460 (1956).